Akhiezer damping in nanostructures

K. Kunal and N. R. Aluru*

Department of Mechanical Science and Engineering, Beckman Institute for Advanced Science and Technology, University of Illinois at Urbana-Champaign, Urbana, Illinois 61801, USA

(Received 12 June 2011; revised manuscript received 14 December 2011; published 30 December 2011)

Dissipation in a nanomechanical resonator under the application of a nearly uniform strain field is investigated using molecular dynamics simulations. Under the application of a uniform strain field and in the frequency range studied, we expect Akhiezer damping to be the dominant loss mechanism. The scaling of energy dissipation rate with frequency for the bulk case and a finite-sized nanostructure are studied and the results are explained by Akhiezer damping. The size effect on the dissipation rate is also investigated. The results show a significant role of the surface on the dissipation rate. An increase in the Q factor with a decrease in thickness of the structure is observed for a certain range. Below some critical thickness, the trend reverses, indicating multiple roles of the surface contributing to the dissipation process.

DOI: 10.1103/PhysRevB.84.245450 PACS number(s): 62.40.+i, 62.80.+f, 63.22.−m, 85.85.+j

I. INTRODUCTION

Nanoresonators, with high resonant frequencies, find a variety of applications such as mass detectors for chemical and biological sensing,[1] transducers, etc. Experimental studies have demonstrated that atomic-scale resolution can be achieved with these mass sensors.[2] The sensitivity of these mass sensors is limited by the quality factor[3] Q, which is defined as the ratio of the energy stored to the energy lost per unit period. A high Q factor or low dissipation rate is required for the high sensitivity of these inertial sensors. Dissipation plays an important role in the stability of nanoelectromechanical systems (NEMS).[4] The Q factor is a design parameter required for predicting the dynamic pull-in voltage of NEMS switches.[5]

The loss of energy in a mechanical resonator can result from different processes, which can be classified into intrinsic and extrinsic dissipation mechanisms. Fluid damping[6] and clamping losses[7,8] are two important extrinsic dissipation mechanisms in a nanoresonator. In the case of an intrinsic dissipation mechanism, the ordered mechanical energy is transformed into the disordered internal energy of the system. Thermoelastic dissipation[9–11] (TED) and Akhiezer damping[12] are two known intrinsic dissipation mechanisms in a single-crystal structure. TED takes place due to the spatial variation of the strain field in a structure, which results in a temperature gradient and, hence, heat flow leading to entropy generation. The Q factor due to TED is given as[9]

$$Q^{-1} = \frac{\alpha^2 E T}{C_v} \frac{\omega\tau_{td}}{1+(\omega\tau_{td})^2}, \tag{1}$$

where C_v is the specific-heat capacity at constant volume, α is the coefficient of thermal expansion, E is the Young's modulus, ω is the angular frequency of oscillation, T is the mean temperature, and τ_{td} is the thermal diffusion time. For a temperature gradient developed across a width w in a material with thermal conductivity κ, $\tau_{td} = \frac{w^2 C_v}{\pi^2 \kappa}$. TED, apart from depending on the material properties, therefore also depends on the length scale across which the temperature gradient is developed.

Akhiezer damping takes place as a result of heat flow between different phonon modes. The applied strain field modulates the frequency of the thermal phonons. The strength of coupling between the strain field and the phonon modes varies and is given by a mode-dependent Grüneisen parameter, which is a measure of the change in frequency of each mode with applied strain. The applied deformation, therefore, results in a temperature difference between different phonon modes, and each of them then tends to relax toward the mean temperature value. This results in an intramode heat flow and, hence, entropy generation leading to dissipation. While TED depends on the applied strain field, Akhiezer damping rate is a more fundamental property of the system. Under the application of a uniform strain field, and in the absence of any additional mechanism of dissipation, the damping rate in a structure will be governed by the Akhiezer mechanism.

Since the original work of Akhiezer,[12] the absorption of acoustic waves by Akhiezer mechanism has been the subject of extensive research. Bommel and Dransfeld[13] developed an expression for attenuation of elastic waves by assuming that the dominant heat flow takes place between two phonon branches. Woodruff and Ehrenreich[14] derived an expression for damping of elastic waves by solving the Boltzmann transport equation. Mason and Bateman[15] introduced a nonlinearity parameter D for the attenuation coefficient due to Akhiezer damping and found good agreement with the experimental results for silicon and germanium. The theories developed in these works have been applied to a number of other experimental works[16,17] wherein it has been demonstrated that the Akhiezer mechanism becomes particularly important when the time scale of oscillation becomes comparable to the phonon relaxation time $\tau_{\text{ph-ph}}$. A metric for assessing the strength of this mechanism is the $\omega\tau_{\text{ph-ph}}$ value. The mechanism plays an important role for the absorption of acoustic waves in the ultrasonic and the hypersonic regimes.

The angular frequency of oscillation of the fundamental longitudinal mode ω_l of a beam is given as

$$\omega_l = \sqrt{\frac{E}{\rho}} \frac{\pi}{2L}, \tag{2}$$

where ρ is the mass density and L is the length of the beam. For L of the order of few nanometers, frequency in the range of tens of GHz is obtained. The phonon relaxation time is

generally of the order of few picoseconds. Thus, for beams with dimension in the range of nanometers, $\omega\tau_{\text{ph-ph}}$ will be of the order of 10^{-2}. The Q factor due to Akhiezer mechanism scales as[13]

$$Q^{-1} \propto \frac{\omega\tau_{\text{ph-ph}}}{1+(\omega\tau_{\text{ph-ph}})^2}. \quad (3)$$

Q attains a minimum value $Q_{\min}$ for $\omega\tau_{\text{ph-ph}} = 1$. For $\omega\tau_{\text{ph-ph}}$ of the order of 10^{-2}, $\frac{Q}{Q_{\min}}$ is of the order of 10^2 and one expects the Akhiezer damping to be an important loss mechanism at such length scales.

A number of experimental as well as theoretical works[18,19] have been carried out to elucidate the dissipation mechanisms in a nanostructure. These works have provided insight into the different possible dynamics operating at the nanoscale. Kiselev *et al.*[20] solved the Boltzmann transport equation and studied the relative importance of TED and Akhiezer damping in a nanobeam under flexure. The analysis, however, did not take into consideration the variation in material properties with size. For example, the value of $\tau_{\text{ph-ph}}$ was assumed to be the same for all sizes. Further attempts to isolate and study the role of individual dissipation dynamics at such small length scales have not been made. A more general study of the role of surface on individual dissipation mechanism is therefore lacking and we attempt to make some effort in this direction.

In this work, we employ classical molecular dynamics (MD) to understand Akhiezer dynamics in nanostructures. The other known dissipation mechanism, namely, TED, is eliminated by applying a nearly uniform strain field. It is worth pointing out that additional mechanisms, such as the surface dissipation, may also be present and mask the dynamics that would have resulted solely from Akhiezer damping. Attempts have not been made to isolate such effects. In Sec. II, we review the dynamics of a beam under longitudinal vibration and present a case of a nearly linear displacement profile. In Sec. III, we describe the MD setup to study the vibration of a nickel nanostructure, using the idea of Sec. II to attain the desired objective. In Sec. IV, the results are summarized, and conclusions are given in Sec. V.

II. BEAM DYNAMICS

The equation of motion for the displacement profile $u(x,t)$ of a purely elastic beam in longitudinal vibration is given by

$$E\frac{\partial^2 u(x,t)}{\partial x^2} + \rho\frac{\partial^2 u(x,t)}{\partial t^2} = f(x,t), \quad (4)$$

where $f(x,t)$ is the applied force. A periodic load $f(x,t) = F_0\delta(x-L)\cos(\omega t)$ is applied at the end where F_0 is the magnitude of the applied load and $\delta(x)$ is the Dirac delta function. The solution of Eq. (4) for such a case is obtained as $u(x,t) = A_m\sin(\frac{\pi x}{2L_0})\cos(\omega t)$. A_m is a measure of the amplitude of oscillation and $L_0 = \frac{\pi}{2\omega}\sqrt{\frac{E}{\rho}}$. The physical interpretation of L_0 is that it corresponds to the length of an imaginary beam, which has the same material properties as stated above and for which the angular frequency of the fundamental longitudinal mode is equal to ω. Under the condition that L is sufficiently smaller than L_0, $u(x,t)$ can be approximated as

$$u(x,t) = A_m\sin\left(\frac{\pi x}{2L_0}\right)\cos(\omega t) \approx A_m\frac{\pi x}{2L_0}\cos(\omega t). \quad (5)$$

This results in a linear displacement profile with a uniform strain field. The amplitude of oscillation at the end of beam A is then given as $A = A_m\frac{\pi L}{2L_0}$. The elastic energy U stored in the beam is given as

$$U = \int_0^L \frac{1}{2}SE\left(\frac{\partial u}{\partial x}\right)^2 dx, \quad (6)$$

where S is the cross-sectional area of the beam.

For a linear displacement profile, U is obtained as

$$U = \tfrac{1}{2}kA^2, \quad (7)$$

where k is the effective stiffness of the beam and is given as $k = \frac{ES}{L}$.

III. SIMULATION SETUP

A nickel structure was generated by arranging atoms on a face-centered cubic (fcc) lattice with a lattice spacing of 3.5374 Å. A schematic of the simulation setup is illustrated in Fig. 1. 20 unit cells, corresponding to a length of 7.07 nm, were taken in the longitudinal [100] direction, while the cross-section area was varied from 3.53×3.53 nm^2 to 7.07×7.07 nm^2 for different studies. All atoms within one unit cell from the left end were fixed by setting the forces on them to be zero. This corresponds to a clamped boundary condition. The embedded atom method (EAM) potential[21] was used to model the force field. Large-scale atomic/molecular massively parallel simulator[22] (LAMMPS) was used for all MD simulations. The structure was equilibrated at 300 K using a Nosé-Hoover thermostat with a time constant of 0.1 ps. A time step of 1 fs was used for the entire simulation. After equilibration of the structure for 2 ns, a periodic force was applied to the atoms on the right longitudinal edge in the x direction. The system was further evolved as a canonical (NVT) ensemble for a simulation time of 30 ns.

For a perfectly elastic structure, the mean displacement of the end atoms would be in phase with the applied periodic force. However, because of dissipation, a phase lag exists between the applied force and the response. The work done by the applied force per unit period is a measure of the energy dissipation rate. In an isolated system (microcanonical ensemble), this work would result in an increase in the internal energy, and hence the temperature, of the system. For a system

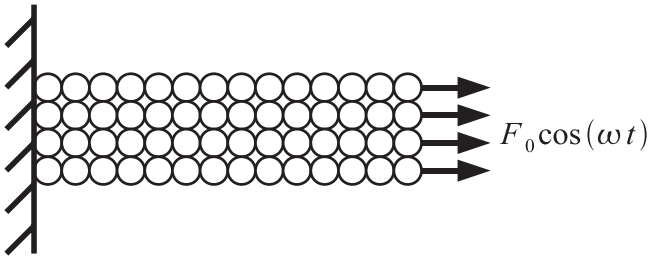

FIG. 1. A schematic of the simulation setup.

evolved as a canonical ensemble, the thermal bath takes away the excess energy and keeps the mean temperature constant. The energy dissipated per unit period E_{diss} is equal to the work done by the external force and is given as

$$E_{\text{diss}} = \frac{\omega}{2\pi T_f} \int_0^{T_f} \sum_{n_e} f_0 \cos(\omega t) v_x dt, \tag{8}$$

where f_0 is the magnitude of the applied force on each of the end atoms, v_x is the x component of the velocity, T_f is the total time for which the force is applied, and n_e is the number of atoms at the end on which the external force is applied. F_0 is related to f_0 as $F_0 = n_e f_0$. We neglected an initial transient of 2 ns from the time the external force was imposed for computing the energy dissipation rate. In order to compute the energy stored, the Fourier transform of the x component of the center-of-mass displacement of the edge atoms was taken. The Fourier transform showed a dominant peak corresponding to the frequency of the applied force. The amplitude of oscillation was computed from the peak magnitude as

$$A = \max\{\text{abs}[\text{FFT}(x\text{-data})]\}/(2\times ndata), \tag{9}$$

where x-data is the time-series data of the center of mass of edge atoms and *ndata* is the number of data points.

The effective stiffness of the structure was determined using a separate equilibrium simulation. After an initial equilibration at 300 K for 2 ns, a static force was applied on the end atoms. The structure was relaxed for 1 ns, the length value corresponding to the applied force was then computed using the data obtained for a subsequent time of 1.5 ns. The force magnitude was then increased and the procedure described above was followed to compute the new relaxed length for the increased applied force value. This was repeated with subsequent force increments and the length value was obtained for different magnitude of the applied force. The slope of the force-displacement curve gives the value of k.

The energy stored E_{stored} was then computed as

$$E_{\text{stored}} = \tfrac{1}{2} k A^2. \tag{10}$$

The Q factor is then given as

$$Q = 2\pi \frac{E_{\text{stored}}}{E_{\text{diss}}}. \tag{11}$$

IV. RESULTS AND DISCUSSION

We first studied the frequency dependence of Q factor for the bulk case. The bulk case was simulated by imposing the periodic boundary condition in the lateral direction. A size independence for a simulation domain with cross-sectional area larger than 3.53×3.53 nm^2 was observed. Figure 2(a) shows the plot of the Q factor versus frequency as obtained for the bulk case. The Q factor decreases and, hence, the dissipation rate increases with the increase in frequency.

Under the single-mode relaxation-time approximation, the Q factor for Akhiezer damping is given as[13]

$$Q^{-1} = \frac{C_p T \lambda_{av}^2}{\rho v^2} \frac{\omega \tau_{\text{ph-ph}}}{1 + (\omega \tau_{\text{ph-ph}})^2}, \tag{12}$$

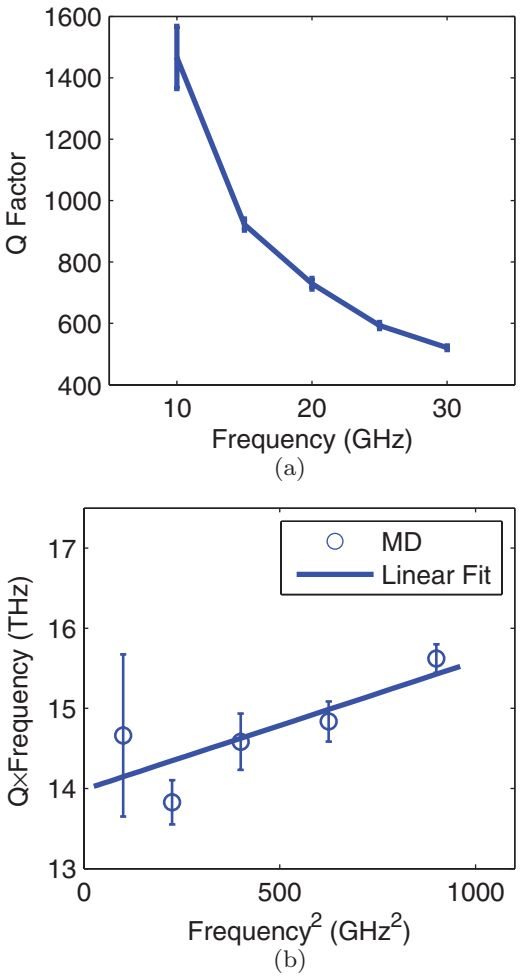

FIG. 2. (Color online) (a) Q factor vs frequency for $7.07 \times 4.24 \times 4.24$ nm nickel structure with periodic boundary condition in the lateral directions. (b) The relaxation relation for the bulk case is illustrated by this plot.

where v is the sound velocity, C_p is the specific-heat capacity at constant pressure, λ_{av} is the mean value of the Grüneisen parameter, ω is the angular frequency of the applied strain field, and $\tau_{\text{ph-ph}}$ is a measure of the phonon energy mean transfer time. Equation (12) states that, for $\omega\tau_{\text{ph-ph}} \leqslant 1$, the Q factor decreases with the increase in frequency. The phonon relaxation time is generally of the order of few picoseconds, and the above inequality is valid if the frequency is of the order of few gigahertz. Equation (12) can be further recasted as

$$Q\omega = m\omega^2 + c, \tag{13}$$

where $m = \frac{\rho \tau_{\text{ph-ph}} v^2}{C_p T \lambda_{av}^2}$ and $c = \frac{m}{\tau_{\text{ph-ph}}^2}$. Equation (13) states that $Q\omega$ and ω^2 have a linear relationship. Figure 2(b) shows the plot of $Q\omega$ versus ω^2 as obtained for the bulk case and a linear dependence between $Q\omega$ and ω^2 is observed. The slope and the intercept of the linear fit were used to compute the $\tau_{\text{ph-ph}}$ value, which was estimated to be 1.72 ps.

Different studies have estimated different values of $\tau_{\text{ph-ph}}$. According to Bommel and Dransfeld,[13] the value of $\tau_{\text{ph-ph}}$

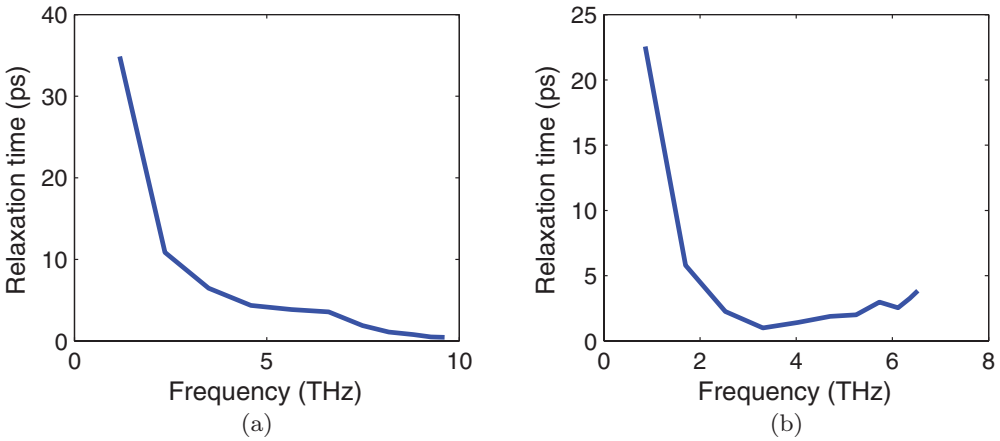

FIG. 3. (Color online) (a) Longitudinal phonon relaxation time for bulk nickel in the [100] direction. (b) Transverse phonon relaxation time for bulk nickel in the [100] direction.

should be taken to be same as that of the thermal relaxation time τ_{th} given as

$$\tau_{\text{th}} = \frac{3\kappa}{C_v v^2}. \tag{14}$$

Mason and Bateman[15] used a value of $\tau_{\text{ph-ph}} = 2\tau_{\text{th}}$ for longitudinal mode and obtained very good agreement with the experimental data. Heino and Ristolainen[23] computed the phonon mean-free path l and v for nickel using MD, although they used a different version of the EAM potential to model the force field. Making use of $\tau_{\text{th}} = \frac{l}{v}$ and using the data given by Heino and Ristolainen,[23] the value of τ_{th} comes out to be 0.96 ps. The ratio $\frac{\tau_{\text{ph-ph}}}{\tau_{\text{th}}} = 1.8$, it then follows that the relation given by Mason and Bateman[15] holds more applicable for our case.

Phonon relaxation time can also be computed by taking the correlation of the mode potential or kinetic energy.[24] $20 \times 10 \times 10$ unit cells of nickel with periodic boundary condition in all directions were used. The relaxation time for phonons in the direction of 20 unit cells, which corresponded to the [100] direction in a fcc lattice structure, is computed at 300 K. A phonon is a propagating wave for which the mode shape is given as

$$\vec{u}_p(\vec{x},t) = \vec{P} \exp\,(i\vec{k}.\vec{x}) \exp\,(i\omega_0 t), \tag{15}$$

where $\vec{x}$ is the position vector of each atom, $\vec{u}_p$ is the displacement from the mean position, $\vec{k}$ is the wave vector, ω_0 is the phonon frequency, and $\vec{P}$ is the polarization vector. $\vec{k}$ is given by the boundary condition. For a given value of $\vec{k}$, one can construct a force constant matrix[25] using second-order derivative of the potential function; the eigenvectors of the force constant matrix then give $\vec{P}$ and the eigenvalues scaled with atomic mass give ω_0^2. $\vec{k}$ and $\vec{P}$ completely characterize a mode shape. MD displacement and velocity are then projected on the mode shape to get the mode displacement d_m and the mode velocity v_m. The mode kinetic energy Ke_m is then computed as $Ke_m = \frac{1}{2}mv_m^2$. The correlation function of Ke_m was taken to estimate the decay rate. Figure 3 shows the relaxation time for the transverse and longitudinal phonons as obtained for the bulk case. The phonon density of states (PDOS) was computed by taking the fast Fourier time (FFT) of the function $C(t)$,[26] given as

$$C(t) = \frac{1}{n_{\text{atoms}}} \left\langle \sum_{n_{\text{atoms}}} \vec{v}_i(t_0).\vec{v}_i(t_0+t) \right\rangle, \tag{16}$$

where n_{atoms} is the total number of atoms and $\vec{v}_i(t)$ is the velocity vector of the ith atom obtained from MD. Figure 4 shows the PDOS obtained for the bulk case using MD. The PDOS has two peaks. The peak at around 6 THz corresponds to the transverse mode, while the peak near 9 THz corresponds to the longitudinal mode. At 5.73 GHz, the transverse mode has a relaxation time of 2.97 ps and at 8.8 GHz the longitudinal mode has a relaxation time of 0.78 ps; the mean of these two values comes to be 1.875 ps, which is comparable to the phonon relaxation time estimated from Q versus ω scaling.

The scaling of Q factor with ω was then studied for the finite-sized case. A free surface boundary condition was imposed in the lateral direction. We considered three different cases, each of them having a length of 7.1 nm in the longitudinal direction, and with cross-sectional areas

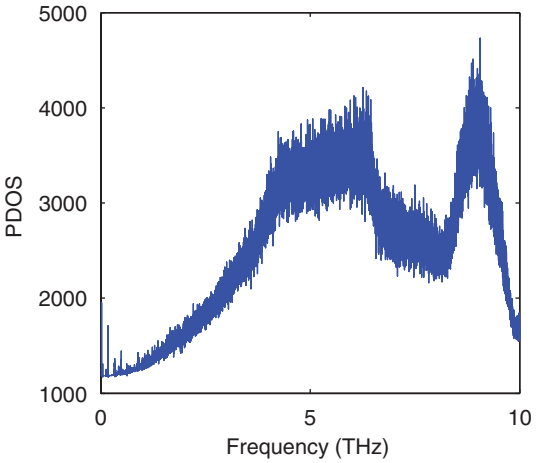

FIG. 4. (Color online) Phonon density of states for bulk nickel.

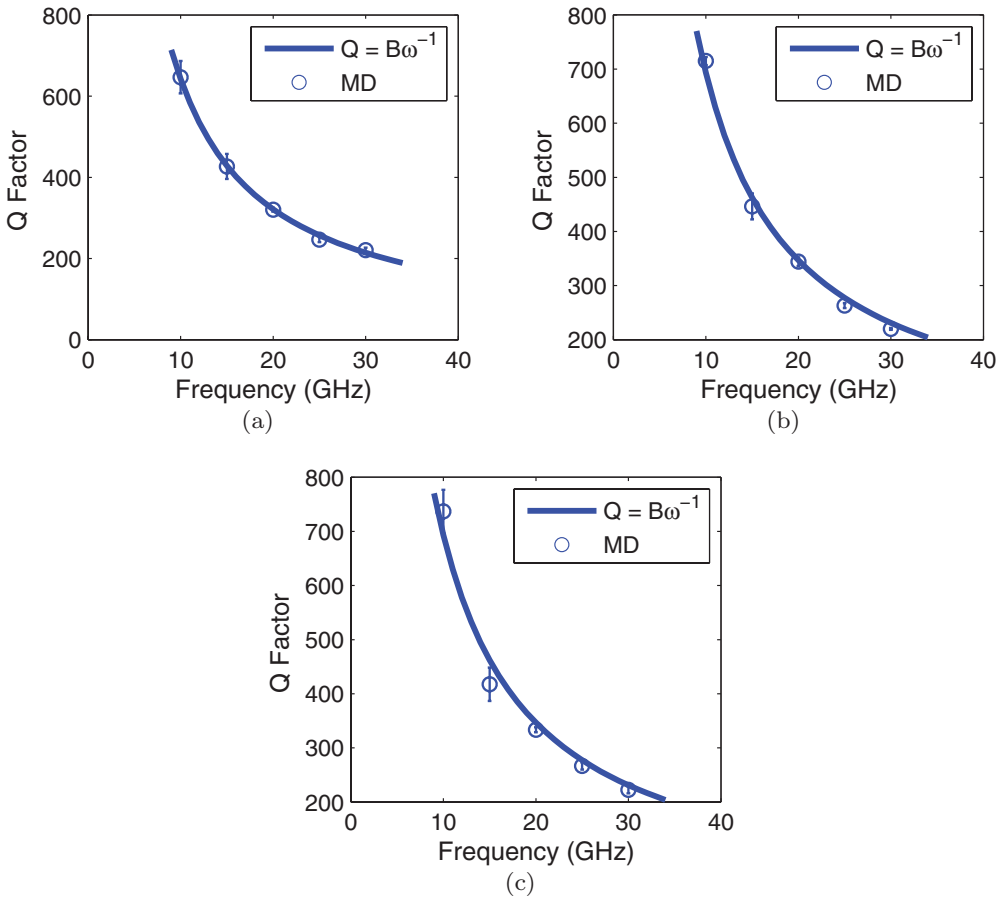

FIG. 5. (Color online) (a) Q factor vs frequency for 7.1×7.1 nm^2 nickel nanostructure. (b) Q factor vs frequency for 5.1×5.1 nm^2 nickel nanostructure. (c) Q factor vs frequency for 3.5×3.5 nm^2 nickel nanostructure.

as 3.53×3.53 nm^2, 5.29×5.29 nm^2, and 7.07×7.07 nm^2. Figure 5 shows the plot of Q versus frequency for the three cases. For all the sizes, the dissipation rate was found to increase with the increase in the frequency. The plot also shows a $Q = B\omega^{-1}$ curve, with B obtained using the least-squares fit from the data points. For the case of cross-sectional area of 7.1×7.1 nm^2, the Q value closely follows the $B\omega^{-1}$ curve. For the smallest size, the MD data and the inverse relationship became slightly deviant. Further, for all three cases, a linear dependence between $Q\omega$ and ω^2, as has been observed for the bulk case, was not seen.

The Q versus ω relation, as stated in Eq. (12), was derived by Bommel and Dransfeld[13] under the assumption that the Grüneisen parameter for a given phonon branch is independent of frequency and two phonon groups are present. This is applicable for a bulk structure for which only the longitudinal and transverse modes are present. In a low-dimensional structure, such as a nanowire, the presence of a surface splits the phonon spectrum into a subband.[27,28] The assumptions used in deriving Eq. (12) are, therefore, not applicable for nanostructures. A linear dependence between $Q\omega$ and ω^2 is, therefore, not observed in the case of free surface boundary condition.

Under the approximation $\omega\tau_{\text{ph-ph}} \leqslant 1$, Woodruff and Ehrenreich[14] derived an expression for damping of elastic waves by solving the Boltzmann transport equation. An expression for the attenuation coefficient α_t was obtained as

$$\alpha_t = \beta \frac{\omega^2 T}{\rho v^2} \sum_{q,j} \tau(q,j)\lambda^2(q,j)C(q,j), \tag{17}$$

where β is a numerical coefficient, and $\tau(q,j)$, $\lambda(q,j)$, and $C(q,j)$ are the relaxation time, the Grüneisen parameter, and specific-heat capacity of the phonon branch labeled as q,j. Q is related to α_t as $Q = \frac{\omega}{2\alpha_t}$ and, hence, Eq. (17) shows that Q scales as ω^{-1}. This explains the trend as has been observed for the case of 7.1×7.1 nm^2 cross-sectional area.

We studied the size dependence of the Q factor for a fixed frequency of 25 GHz. The cross-sectional area was varied from 12.51 to 50.41 nm^2. Figure 6 shows that the Q factor first shows an improvement with the decrease in size and then drops below some critical size. This trend in the variation of Q factor with size indicates the role of different competing factors.

The initial decrease in the dissipation rate with the decrease in size can be explained by the role of surface on the ensemble of thermal phonons. Akhiezer damping takes place as a result of the modulation of thermal phonons with the applied strain field. The strain field disturbs the equilibrium of the thermal phonons, which then relax toward equilibrium with a finite relaxation time. Faster relaxation of phonons toward thermal equilibrium would decrease the lag between the stress and

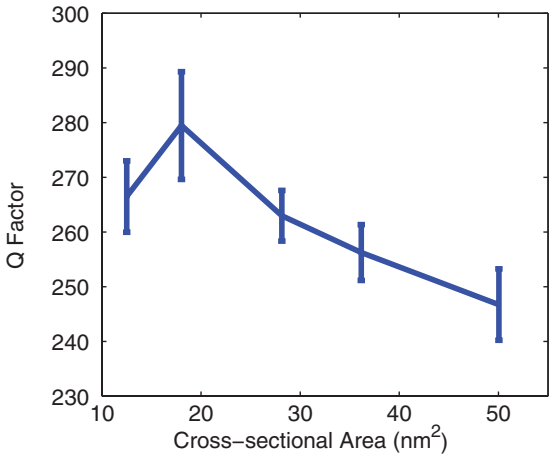

FIG. 6. (Color online) Variation of Q factor with cross-sectional area for square nickel beam with a length of 7.1 nm at 25 GHz.

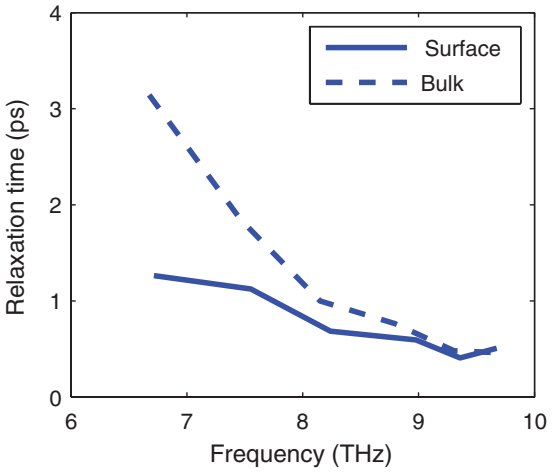

FIG. 7. (Color online) Relaxation time for longitudinal phonons in nickel nanowire and its comparison with bulk value.

the strain and would result in a lower dissipation rate. A manifestation of this effect was observed by Harding and Wilks,[29] who found that the attenuation of sound in liquid helium decreased by the addition of a small amount of ^{3}He impurity. The presence of surfaces acts as an additional scattering mechanism[30,31] and reduces the relaxation time of thermal phonons in nanostructures. Such an effect has been studied before and has been accounted for as a reason for the decrease in the thermal conductivity of nanowires.[32]

The phonon relaxation time for a finite-sized case was computed using the method described by McGaughey and Kaviany.[24] A nickel structure with $20 \times 12 \times 12$ unit cells ($7.1 \times 4.24 \times 4.24$ nm) was used with a periodic boundary condition in the direction of 20 unit cells and a free surface boundary condition in the other directions. Computing the phonon relaxation time in this case would entail using the eigenmodes for the one-dimensional structure. The mode shapes were computed using the method described before for the case of bulk system. For large wave vectors, the bulk modes corresponded to the eigenmodes of the structure considered. This was evident from the correlation function of the mode potential or kinetic energy, which showed a dominant single frequency. The relaxation time was computed only for large wave vectors for which the eigenmodes are sufficiently given by the bulk mode shapes. Figure 7 shows the plot of relaxation time for longitudinal phonons as obtained for the finite-sized case. The bulk values are also plotted for comparison. For the higher-frequency values, both the finite structure and bulk have similar relaxation time. In this case, the relaxation is dominated by the umklapp process. The relaxation time deviates with the decrease in frequency, with the finite-size case having a lower value. The presence of surfaces therefore reduces the mean phonon relaxation time.

The autocorrelation function $S(t)$ of the heat current vector $\vec{q}(t)$ can be used to estimate phonon mean relaxation times.[33] For a fcc crystal, $S(t)$ shows a two-stage decay. A biexponential fit of $S(t)$ gives two relaxation times.[34] The relaxation time with the smaller value is the mean lifetime of short-wavelength phonons τ_{sp}. Physically, τ_{sp} corresponds to the time an atom takes to transfer energy to its neighboring atoms. The second relaxation time obtained from the biexponential fit is the long-wavelength phonons mean lifetime τ_{lp}.

τ_{sp} and τ_{lp} values were estimated for nickel nanowires of varying cross-sectional area. The periodic boundary condition was used in the longitudinal direction, while the free surface boundary condition was used otherwise. $S(t)$ was computed by taking the autocorrelaton of the component of $\vec{q}(t)$ in the longitudinal direction. A total simulation time of 6 ns was used to compute $S(t)$. The biexponential fitting was done on the values of $S(t)$ for a period of 5 ps. τ_{sp} was estimated to be of the order of a few femtoseconds. For the frequency range under consideration, this time scale is not of importance and hence was not considered for analysis. Figure 8 shows the τ_{lp} values for different cross-sectional areas. The plot shows that τ_{lp} decreases with the decrease in size. This decrease in τ_{lp} value with the decrease in size is expected to govern the Q-factor variation for larger sizes. For the Akhiezer mechanism, dissipation rate and relaxation time have a direct relationship and, hence, the dissipation rate initially decreases with the decrease in size.

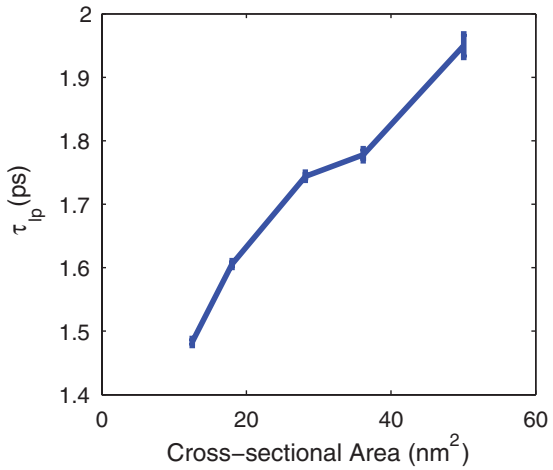

FIG. 8. (Color online) Variation of the long-wavelength phonons mean relaxation time τ_{lp} with size.

The surface atoms, because of lower coordination number, have intrinsic properties that are different from the bulk atoms. The increasing role of surface atoms, with the increase in surface to volume ratio, results in change in the properties of a nanostructure. The length scale at which such an effect becomes important is of the order of a few nanometers. The magnitude of this length scale depends on the material property of interest and the nature of the material itself. For example, the Young's modulus of a silicon nanowire drops sharply below a cross-section area of 10 nm^2.[35]

The physical origin of the Akhiezer damping mechanism lies in the flow of heat current between different phonon modes. The flow of heat takes place due to the difference in $\lambda(q,j)$ values between different modes, with $\lambda(q,j)$ being a measure of the change in temperature of each mode when strained adiabatically. The higher the difference in the $\lambda(q,j)$ value for different modes, the higher will be the temperature difference. This effect on the dissipation rate is quantified by a nonlinearity parameter[15] D given as

$$D = 3\left[\frac{3\sum_{q,j}[\lambda^2(q,j)]}{n} - \frac{\lambda^2 C_v T}{E_0}\right], \tag{18}$$

where n is the number of the modes, E_0 is the total thermal energy, and λ is the volume Grüneisen constant. The attenuation due to the Akhiezer mechanism is related to D as $\alpha_t = \frac{D\omega^2 E_0 \tau_{\text{ph-ph}}}{6\rho v^3}$.

D by definition is therefore a metric of the variance in the $\lambda(q,j)$ value. In a bulk crystal, the main contribution to D comes from the difference in the $\lambda(q,j)$ value between the transverse and the longitudinal branches. The presence of surface leads to additional modes in a nanostructure. Some of these modes, called the surface modes, have displacement profiles in which the surface atoms share most of the amplitude. $\lambda(q,j)$ for such modes will therefore depend on the property of the surface atoms and will be different from that of the bulklike modes. The presence of such modes will therefore contribute to an increase in the value of D and, hence, an increase in the dissipation rate. The fraction of such modes to the total number of modes depends on the ratio of the number of surface atoms to that of the bulk atoms and is expected to become significant only at very small dimension.

The local quasiharmonic (LQHM) model[36] was used to estimate the D value for nickel nanobeams. In the LQHM model, the motion of each atom is decoupled from the rest. A local stiffness matrix $\Phi(\alpha)$ is obtained by taking the double derivative of the potential energy with respect to displacement vector of an atom α. From the eigenvalues of $\Phi(\alpha)$, three vibrational frequencies $\omega_{\alpha i}(i = 1,2,3)$ are determined. The local Grüneisen parameter $\lambda_{\alpha i}$ is given as $\lambda_{\alpha i} = -\frac{V}{\omega_{\alpha i}}\frac{d\omega_{\alpha i}}{dV}$, where V is the volume of the crystal. We define $C_{\alpha i}$ as $C_{\alpha i} = \frac{k_b(\frac{\hbar\omega_{\alpha i}}{k_b T})^2 \exp(\frac{\hbar\omega_{\alpha i}}{k_b T})}{[\exp(\frac{\hbar\omega_{\alpha i}}{k_b T})-1]^2}$ and $E_{\alpha i}$ as $E_{\alpha i} = \frac{\hbar\omega_{\alpha i}}{\exp(\frac{\hbar\omega_{\alpha i}}{k_b T})-1}$, where k_b is the Boltzmann constant, $\hbar = \frac{h}{2\pi}$, and h is the Plancks constant. In the LQHM model, λ is obtained as

$$\lambda = \frac{\sum_{\alpha=1}^{\text{nt}}\sum_{i=1}^{3} C_{\alpha i}\lambda_{\alpha i}}{\sum_{\alpha=1}^{\text{nt}}\sum_{i=1}^{3} C_{\alpha i}}, \tag{19}$$

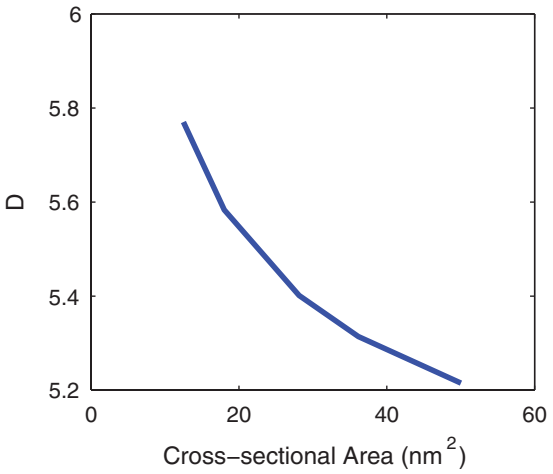

FIG. 9. (Color online) Variation of the nonlinearity parameter D with size as computed using the LQHM model.

where nt is the total number of atoms in the structure. C_v and E_o in the LQHM model are given as $C_v = \frac{1}{V}\sum_{\alpha=1}^{\text{nt}}\sum_{i=1}^{3} C_{\alpha i}$ and $E_0 = \frac{1}{V}\sum_{\alpha=1}^{\text{nt}}\sum_{i=1}^{3} E_{\alpha i}$.

Finite-sized nickel nanostructrues, as used in the MD simulations, were considered for LQHM analysis. $\lambda_{\alpha i}$ values were computed by imposing a uniaxial deformation on the structure. The values of $\lambda_{\alpha i}$, λ, C_v, and E_0 thus obtained using the LQHM model were substituted in Eq. (18) to get the value of D. Figure 9 shows the value of D for nickel nanobeams of different cross-sectional area. The plot shows that D increases with the decrease in size. For the smallest size considered, the increase in the value of D is expected to become significant and compensate for the decrease in the relaxation-time value. This effect of surface on the D value plausibly explains the observed nonmononotic scaling of the Q factor with size.

V. CONCLUSIONS

MD simulations have been used to investigate the dissipation in a nickel nanowire. A nearly uniform strain field was applied to eliminate TED. In such a case, we expect the dissipation to be dominated by the Akhiezer mechanism. From the scaling of the Q factor with ω for the bulk case, $\tau_{\text{ph-ph}}$ was estimated. The value was comparable with the estimate obtained from other methods. The finite-sized case showed an inverse scaling of Q factor with ω, and for the smallest size considered, a slight deviation was observed. The size dependence of the Q factor showed a positive role of the surface wherein the Q factor initially increased with the decrease in thickness. This was explained by the role of the surface as a scattering medium for the thermal phonons. For dimensions below some critical value, a drop in Q factor with size was observed, and this was attributed to the contribution of surface atoms to increase the variance in the $\lambda(q,j)$ value.

ACKNOWLEDGMENT

This research was supported by NSF under Grants No. 0941497 and No. 1127480.

*aluru@illinois.edu

[1]B. Ilic, Y. Yang, K. Aubin, R. Reichenbach, S. Krylov, and H. G. Craighead, Nano Lett. **5**, 925 (2005).
[2]K. Jensen, K. Kim, and A. Zettl, Nat. Nanotechnol. **3**, 1038 (2008).
[3]K. L. Ekinci, Y. T. Tang, and M. L. Roukes, J. Appl. Phys. **95**, 2682 (2004).
[4]N. Pugno, Glass Phys. Chem. **31**, 535 (2005).
[5]N. Pugno, C. H. Ke, and H. D. Espinosa, J. Appl. Mech. **72**, 445 (2005).
[6]R. B. Bhiladvala and Z. J. Wang, Phys. Rev. E **69**, 036307 (2004).
[7]G. D. Cole, I. W-Rae, K. Werbach, M. R. Vanner, and M. Aspelmeyer, Nat. Commun. **2**, 231 (2011).
[8]J. H. Ko, J. Jeong, J. Choi, and M. Cho, Appl. Phys. Lett. **98**, 171909 (2011).
[9]C. Zener, Phys. Rev. **53**, 90 (1938).
[10]R. Lifshitz and M. L. Roukes, Phys. Rev. B **61**, 5600 (2000).
[11]S. K. De and N. R. Aluru, Phys. Rev. B **74**, 144305 (2006).
[12]A. Akhiezer, J. Phys. (Moscow) **1**, 277 (1939).
[13]H. E. Bommel and K. Dransfeld, Phys. Rev. **117**, 1245 (1960).
[14]T. O. Woodruff and H. Ehrenreich, Phys. Rev. **123**, 1553 (1961).
[15]W. P. Mason and T. B. Bateman, J. Acoust. Soc. Am. **36**, 644 (1964).
[16]M. F. Lewis, J. Acoust. Soc. Am. **43**, 852 (1968).
[17]S. D. Lambade, G. G. Sahasrabudhe, and S. Rajagopalan, Phys. Rev. B **51**, 15861 (1995).
[18]R. Lifshitz, Phys. B (Amsterdam) **316**, 397 (2002).
[19]P. Mohanty, D. A. Harrington, K. L. Ekinci, Y. T. Yang, M. J. Murphy, and M. L. Roukes, Phys. Rev. B **66**, 085416 (2002).
[20]A. A. Kiselev and G. J. Iafrate, Phys. Rev. B **77**, 205436 (2008).
[21]S. M. Foiles, M. I. Baskes, and M. S. Daw, Phys. Rev. B **33**, 7983 (1986).
[22]S. Plimpton, J. Comput. Phys. **117**, 1 (1995).
[23]P. Heino and E. Ristolainen, Microelectron. J. **34**, 773 (2003).
[24]A. J. H. McGaughey and M. Kaviany, Phys. Rev. B **69**, 094303 (2004).
[25]H. Zhao, Z. Tang, G. Li, and N. R. Aluru, J. Appl. Phys. **99**, 064314 (2006).
[26]W. Weber, Phys. Rev. B **15**, 4789 (1977).
[27]P. Hepplestone and G. P. Srivastava, Phys. Status Solidi **1**, 2617 (2004).
[28]M. A. Stroscio and M. Dutta, *Phonons in Nanostructure* (Cambridge University Press, Cambridge, 2001).
[29]G. O. Harding and J. Wilks, Proc. R. Soc. A **268**, 424 (1962).
[30]M. G. Holland, Phys. Rev. **132**, 2461 (1962).
[31]G. P. Srivastava, *The Physics of Phonons* (IOP Publishing, Bristol, 1980).
[32]J. Zou and A. Balandin, J. Appl. Phys. **89**, 2932 (2001).
[33]D. A. McQuarrie, *Statistical Mechanics* (University Science Books, Sausalito, CA, 2000).
[34]A. J. H. McGaughey and M. Kaviany, Int. J. Heat Mass Transfer **47**, 1783 (2004).
[35]Z. Tang and N. R. Aluru, Phys. Rev. B **74**, 235441 (2006).
[36]Z. Tang, H. Zhao, G. Li, and N. R. Aluru, Phys. Rev. B **74**, 064110 (2006).